

Visual Concept-driven Image Generation with Text-to-Image Diffusion Model

Tanzila Rahman^{1,3} Shweta Mahajan^{1,3} Hsin-Ying Lee² Jian Ren²
 Sergey Tulyakov² Leonid Sigal^{1,3,4}

¹University of British Columbia ²Snap Inc.
³Vector Institute for AI ⁴Canada CIFAR AI Chair

Abstract. Text-to-image (TTI) diffusion models have demonstrated impressive results in generating high-resolution images of complex and imaginative scenes. Recent approaches have further extended these methods with personalization techniques that allow them to integrate user-illustrated concepts (e.g., the user him/herself) using a few sample image illustrations. However, the ability to generate images with multiple interacting concepts, such as human subjects, as well as concepts that may be entangled in one, or across multiple, image illustrations remains illusive. In this work, we propose a concept-driven TTI personalization framework that addresses these core challenges. We build on existing works that learn custom tokens for user-illustrated concepts, allowing those to interact with existing text tokens in the TTI model. However, importantly, to disentangle and better learn the concepts in question, we jointly learn (latent) segmentation masks that disentangle these concepts in user-provided image illustrations. We do so by introducing an Expectation Maximization (EM)-like optimization procedure where we alternate between learning the custom tokens and estimating (latent) masks encompassing corresponding concepts in user-supplied images. We obtain these masks based on cross-attention, from within the U-Net parameterized latent diffusion model and subsequent DenseCRF optimization. We illustrate that such joint alternating refinement leads to the learning of better tokens for concepts and, as a by-product, latent masks. We illustrate the benefits of the proposed approach qualitatively and quantitatively with several examples and use cases that can combine three or more entangled concepts.

Keywords: Diffusion model · Segmentation · Concept-driven generation

1 Introduction

Photorealistic image synthesis, particularly with text-to-image diffusion models (*e.g.*, Stable Diffusion [46]), has provided a great boost to content creation. Images of diverse and imaginative scenarios such as “*A dog in space*” can now be easily generated. While such approaches can faithfully generate many instances of the generic subject, *e.g.*, a *dog*, in a variety of scenarios, *e.g.*, *space*, they are limited when the goal is to render a specific subject, *e.g.*, my Beagle dog Bailey

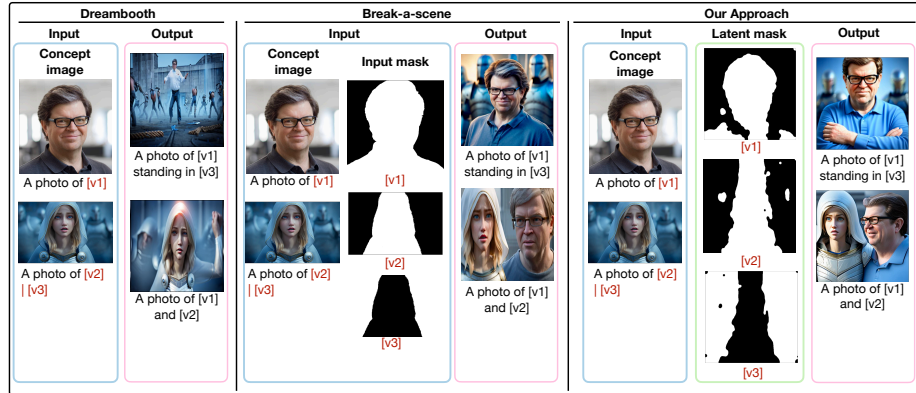


Fig. 1: Concept-driven image generation: Given images depicting multiple concepts (*subjects and context/background*), the top output is the illustration of the male ([v1]) being generated in the context/background of the female ([v3]) image by different methods. The bottom output illustrates the two concepts together in a single image. Dreambooth [47] (left) encodes [v1], [v2], [v3] from multiple input concept images. It fails to generate multi-concept interactions. Break-a-scene [4] (middle) disentangles [v1], [v2], [v3] from single image. This approach requires human-annotated masks. Our approach (right) disentangles [v1], [v2], [v3] from single image. The *latent masks* are obtained from EM-like optimization. Using these optimized masks, our method can automatically produce images with those concepts in new contexts either by themselves or, jointly, interacting with one another.

with unique fur markings, in a specific context or background, *e.g.*, next to my Tudor-style house. Further, the generative capabilities fall apart when modeling multi-object scenarios and interactions, *e.g.*, me playing with Bailey next to my house. Since these cases are frequent and typical in visual content creation, such as stories or videos, it is useful to consider how to make existing text-to-image diffusion models more controllable and capable of generating multiple interacting user-specified concepts. To introduce additional controllability, for example, concerning subject appearance or style and their occurrence in different contexts, many recent approaches [13, 18, 47, 57] have focused on controlling generation with sample images depicting concepts of interest. For example, to render a specific subject, these approaches present multiple (usually relatively clean) images of the target subject to extract the single subject-specific token across these images, *e.g.*, using inversion techniques, and then introduce this special token in prompts in conjunction with the regular text to generate desired content. However, while one can generate single concept/subject scenarios in this way, composing *multiple* stylistically diverse concepts remains a challenge.

Consider images in Fig. 1; approaches discussed above are capable of extracting the specific subject (from the left concept images) and “pasting” them in different contexts. However, they have shown to be significantly limited [4] when asked to generate images where, for example, two characters in question

interact or when multiple concepts come from the same image (*e.g.*, the top-left image can be the source of both the *subject* and the *background*). Learning of tokens and subsequent generation, in this scenario, requires explicit *disentanglement* of the characters and the background. Further, stylistic variations (top – game rendering; bottom – real photograph) present added challenges.

To address these limitations, recent work [4] proposes a two-stage training pipeline for extracting multiple concepts from a single image by leveraging a user-specified mask for each of the concepts during the optimization of tokens associated with these concepts. This mechanism enables the decomposition of an image into constituent subjects and the background. Analogous to prior methods that use multiple images to learn a single concept, this approach also learns how to encode features of each of the concepts into corresponding tokens. A key feature of the pipeline lies in the fine-tuning of model weights while optimizing the prompts for different concepts simultaneously. This ensures that multiple concepts can be compositionally combined. While this works well in practice, the process requires users to specify masks for concepts they desire, which requires a custom sketching interface and additional user effort (as shown in Fig. 1, middle).

In this work, we attempt to do away with the need to specify masks for multi-concept extraction and composition, while still leveraging (latent) masking to learn disentangled concepts that can then be composed using the text-to-image diffusion model [46]. Specifically, we utilize loose textual input prompts and the cross-attention maps for the target concept tokens to generate masks during prompt optimization. However, generating concept masks from cross-attention (*e.g.*, as is done in [54]) of pre-trained diffusion model tends to be noisy; often under- or over-segmenting the target concept(s). Therefore, we propose a joint EM-style optimization over the concept tokens and their (latent) masks, where given mask initializations (obtain in the style of [54] from cross-attention) we iterate between learning tokens for masked concepts and re-estimation of the mask itself. We illustrate that this leads to both learning of better concept tokens and, as a by-product, a better latent mask for the concepts in question.

As is illustrated in Fig. 1 the proposed approach can automatically learn tokens corresponding to the two subjects ([v1], [v2]) and their backgrounds. Given these tokens, it can seamlessly integrate subject in [v3] within the environment of [v2] and can also generate plausible interactions between the two subjects. Note that it can do so despite stylistic differences between the concept sources. Our contributions are:

- We address a unique and challenging problem of personalized multi-subject generation with complex interactions of (potentially unrelated) subjects.
- We propose an Expectation Maximization (EM)-like optimization procedure to disentangle concepts from a single, or multiple, images by generating masks for specific target concepts. Our approach performs token optimization while simultaneously optimizing corresponding (latent) masks such that the token embedding best represents the disentangled concept.
- We show through novel combinations of subjects and interactive environments that our approach works well in practice and can generate realistic

scenarios with custom subjects interacting in complex scenes and environments.

2 Related Work

Image and text-to-image generation. Realistic and high-quality image synthesis is now possible with the outstanding advances in deep generative models. Generative Adversarial Networks (GANs) [1–3, 5, 13, 14, 25, 26, 33] facilitate the creation of high-fidelity images spanning different domains. In addition to GANs, Variational Autoencoders (VAEs) [29, 50] have presented a likelihood-based method for generating images. Important class of generative models include autoregressive models [8, 11, 40, 41] and diffusion models [6, 10, 21, 22, 38, 46, 48]. The former views image pixels as a sequence with pixel-by-pixel correlation, while the latter generates images by gradually removing noise. Methods such as DALL-E [44] employed an autoregressive transformer [51] trained on both text and image tokens, showcasing remarkable zero-shot capabilities.

Diffusion-based models [21] with their spectacular realistic synthesis capabilities have risen as the leading choice for generating images from text descriptions [16, 20, 27, 28, 43, 56]. Some notable works on conditional diffusion models include GLIDE [37] which applies classifier and classifier-free guidance strategies for high-fidelity image generation. Methods such as LAFITE [59] used a pre-trained CLIP [42] model to create a unified space for both text and images, enabling the training of text-to-image models without relying on specific textual datasets. While these approaches were applied directly in the high-dimensional space of images, recent work, Latent Diffusion Model (LDM) [46] for text-to-image generation apply diffusion to a low-dimensional visual representation and have, thus, reduced the computational overhead of the diffusion models applied in the image space. In this work, we build on latent diffusion models.

Personalizing image generation. Personalization involves identifying a concept provided by the user that is not commonly found in the training data for discriminative [9] or generative [39] purposes. Current approaches for customized text-to-image generation with diffusion models have focussed on two types of strategies. In the first, methods [7, 12, 19, 31, 36, 47] adopt test-time fine-tuning where model weights are updated using a collection of images representative of the target concept/subject for personalization. The second strategy is to focus solely on refining the token embedding representing the subject while keeping the model weights fixed to enhance the model’s comprehension of visual concepts [13, 18, 57]. In this direction, DreamBooth [47] takes a holistic approach by fine-tuning the entirety of the UNet network. In contrast, Custom Diffusion [31] concentrates its fine-tuning efforts exclusively on the K and V layers within the UNet network’s cross-attention mechanism. This fine-tuning process is then optimized using LoRA [23]. Conversely, SVDiff [19] pioneers the use of cut mix to construct training data and introduces regularization penalties to mitigate

overlapping attention maps associated with multiple subjects during the training process. Cones [35] introduces the notion of concept neurons and exclusively modifies these neurons related to a specific subject within the K and V layers of cross-attention. To generate multiple personalized subjects, Cones directly combines the concept neurons from several trained personalized models. In contrast, Mix-of-Show [17] adopts a different approach by training individual LoRA models for each subject and subsequently merging their outputs through fusion techniques. In this work, we explore the integration of subjects extracted from multiple images, examining their mutual influence to generate images driven by these subjects. We utilize cross-attention maps to disentangle acquired subjects by optimizing masks.

Inversion in generative models. Inversion tasks in generative models involve identifying a latent code, typically within the latent space of a generative model, that can faithfully recreate a specific image [55, 61]. The process of inversion is achieved either through optimization-based methods that directly refine a latent vector [1, 15, 62] or by employing an encoder to discern and generate the latent representation corresponding to a given image [45, 49, 60]. In this work, we adhere to the optimization method, considering its superior adaptability to novel or unfamiliar concepts. The work incorporates a dual-phase strategy. Initially, we optimize solely the textual embeddings related to the target concepts using masks generated by cross-attention maps. Subsequently, we undertake joint training, refining both the embeddings through mask optimization and the model weights simultaneously.

3 Methodology

To generate images with user-specified concepts (subjects or background) and enable interactions between multiple such concepts and in various contexts, it is essential to extract the concept information, disentangle its specific visual representation, and encode it in the diffusion model. We define a *concept* as a visually illustrated instance of an object/subject or a well exemplified pattern. Note that such concepts often entangle content and style. Diffusion models encode the textual guidance for accurate image generation through cross-attention between the textual tokens and the corresponding region in the image. Therefore, to associate *new* tokens with particular concepts, a masked representation of the target image highlighting only the specific concept is inevitably beneficial. We consider an alternating expectation maximization (EM) style optimization to jointly learn: the tokens – encoding the concept-specific information; and the binary masks – corresponding to each concept of interest. This methodology provides for accurate reconstruction of the target concept in arbitrary contexts, even when involving complex interactions between the subjects. In the following, we first introduce the backbone and the constituent components of our optimization framework.

Latent diffusion model. Latent Diffusion Models (LDM) [46] use perceptual image compression to project the original image to a lower-dimensional space. An

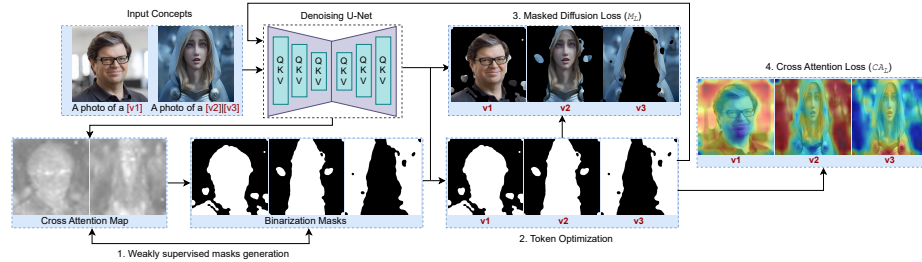


Fig. 2: Overview of our EM-style Optimization Framework. Unique tokens are first assigned to the concepts. In this example, three tokens are assigned: $[v1]$ to the male subject in the first image, $[v2]$ to the female subject in the second image, and $[v3]$ to the background in the second image. Where appropriate these tokens could be initialized with CLIP text embeddings semi-representative of the concept (e.g., “person” for both $[v1]$ and $[v2]$) or simply initialized with random vector embeddings. The latent masks are then initialized by averaging cross-attention maps (see left of Step 1) between the newly defined tokens and the corresponding images across randomly selected 50 diffusion timesteps. The resulting attention maps are subsequently binarized and refined using DenseCRF, resulting in latent binary masks (see right of Step 1). In Step 2, the tokens are re-optimized for a newly sampled timestep with a combination of Mask Diffusion Loss (3) and Cross-Attention Loss (4) [see text for details]. The new tokens are then used to refine cross-attention and the mask. This alternating optimization continues for a fixed number of steps until masks and tokens converge.

encoder $E(\cdot)$ maps the input image $\mathbf{I} \in \mathbb{R}^{H \times W \times 3}$ to a latent representation $\mathbf{Z} \in \mathbb{R}^{h \times w \times c}$, downsampling the image to a lower spatial dimension. The diffusion model is then applied to the latent \mathbf{Z} , where a time-conditioned U-Net $\epsilon_\theta(\mathbf{Z}_t, t)$ models the diffusion process. The objective of the latent diffusion model is,

$$\mathcal{L}_{LDM} := \mathbb{E}_{t, \mathbf{Z}, \epsilon} [\|\epsilon - \epsilon_\theta(\mathbf{Z}_t, t)\|_2^2]. \quad (1)$$

Mask extraction. Following [54], we leverage the cross-attention maps to generate the mask of the target concept. Given a conditioning prompt $\mathbf{y} \in \mathbb{R}^{N \times d}$ where N is the number of tokens in the prompt and d is the embedding dimension, a cross-attention layer with key (\mathbf{K}), query (\mathbf{Q}) and value (\mathbf{V}) is given by,

$$\mathbf{A} = \text{softmax} \left(\frac{\mathbf{Q}\mathbf{K}^T}{\sqrt{d}} \right) \cdot \mathbf{V}. \quad (2)$$

The attention map \mathbf{A}^1 can be reshaped to $H \times W \times N$ such that each slice $\mathbf{A}_p \in \mathbb{R}^{H \times W}$ represents the region attended by the p^{th} token. These attention maps are averaged across all layers of the U-Net to get the response for the

¹ Here, $\mathbf{Q} = \mathbf{W}_Q \cdot \hat{f}(\mathbf{Z})$, $\mathbf{K} = \mathbf{W}_K \cdot f(\mathbf{y})$ and $\mathbf{V} = \mathbf{W}_V \cdot f(\mathbf{y})$, and $\mathbf{W}_Q \in \mathbb{R}^{d \times d_q}$, $\mathbf{W}_K \in \mathbb{R}^{d \times d_k}$ and $\mathbf{W}_V \in \mathbb{R}^{d \times d_v}$ are learnable parameters, $\hat{f}(\mathbf{Z})$ an intermediate flattened feature representation of \mathbf{Z} within the diffusion model and $f(\mathbf{y})$ the feature representation of the condition \mathbf{y} .

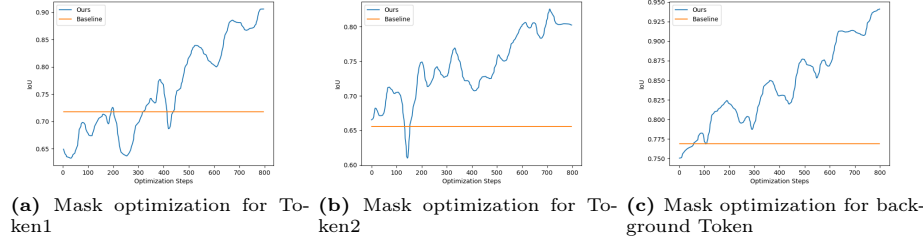


Fig. 3: Quantitative comparison - Mask IoU as a function of training steps. We compare the estimated (latent) mask and the manually annotated mask for the concepts illustrated in Figure 1. Performance, as a function of mask optimization, for different tokens over training steps is illustrated: (a) Mask optimization for [v1] (i.e. *subject*), (b) Mask optimization for [v2] (i.e. *another subject*), and (c) Mask optimization for [v3]. The yellow line indicates a baseline where the mask is obtained once and not updated jointly with the tokens (hence fixed value). A clear trend of improvement is observed for all masks. Curves are smoothed to highlight trends.

regions attended by the target tokens. Note that the latent diffusion objective and hence the attention map are a function of the timestep t . Therefore the quality of the mask would in general differ depending on one or a range of timesteps considered. We will discuss this in more detail later.

To obtain the binary mask \mathbf{B} , we follow the simple process of using a fixed threshold and assigning a value of 1 for pixel values larger than the threshold and 0 otherwise. We further refine the binary masks using the dense conditional random field (DenseCRF) [30], where a DenseCRF, or fully connected CRF, endows pairwise potentials for each pair of pixels in an image where the local relationship, which is based on the color and distance of pixels. The goal of CRF optimization is to satisfy the soft unary constraints obtained by passing a stack of binary masks for each image through a `softmax`, while attempting to ensure nearby and similar pixels are assigned the same class label. It yields refined segmentation that respects natural segment boundaries in the image, which we call \mathbf{M} . We adopt DenseCRF hyperparameters from CutLER [52].

Masked diffusion loss. The input prompt for token optimization is designed such that it contains tokens for target concepts. In a prompt \mathbf{y} with k tokens of interest, diffusion loss is applied to the corresponding pixels which in turn are obtained from the binary mask of each token. Therefore, considering $\mathcal{M}_k = \bigcup_{i=1}^k \mathbf{M}_i$ to the union of the pixels of k concepts, the masked diffusion loss [4] is given by,

$$\mathcal{L}_{Mask} := \mathbb{E}_{t, \mathbf{Z}, \epsilon} \left[\|\epsilon \odot \mathcal{M}_k - \epsilon_\theta(\mathbf{Z}_t, t) \odot \mathcal{M}_k\|_2^2 \right]. \quad (3)$$

Cross attention loss. The masked diffusion loss attends to all the desired concept tokens in a prompt. To enforce that a single token encodes information specific to its corresponding instance, we also include the cross-attention loss [4] which

encourages the token to attend to only the corresponding target concept,

$$\mathcal{L}_{attn} := \mathbb{E}_{i, \mathbf{Z}, t} [\|C_{attn}(\mathbf{Z}_t, \mathbf{y}_i) - \mathbf{M}_i\|_2^2]. \quad (4)$$

Here, $C_{attn}(\cdot)$ is the cross-attention map between the visual representation \mathbf{Z}_t at timestep t and the token \mathbf{y}_i in prompt \mathbf{y} with k concepts, and \mathbf{M}_i is the (latent) mask for token \mathbf{y}_i .

Optimization. To ensure that the tokens learned correspond to the target concept, we introduce binary masks to constrain the loss during prompt optimization and update the tokens under the mask. We adopt a weakly supervised approach and an alternating optimization procedure for learning the concepts. An EM optimization leads to better convergence under good initialization of the parameters.

To obtain a reasonable initial estimate of the token embeddings of specific concept-tokens and their corresponding masks, in the first stage, we perform the following updates: We first obtain initial concept token embeddings by either initializing them from CLIP or by performing inversion without masking to optimize the tokens for a fixed number of iterations. This provides us with good initial token embeddings. With these initial token embeddings at hand, we initialize the masks by following the steps outlined in mask extraction and average the masks over certain timesteps to reduce the errors introduced by stochasticity.

In the second stage, given good initializations of the tokens and their masks, we perform an alternating update of the tokens given the masks and of the masks themselves. Using Eq. (3) and Eq. (4), we first optimize the prompt given the masks for each concept at the iteration. In the following step, for the optimized token, we compute the Eq. (3) to update the mask (from cross-attention). Finally, we optimize the tokens and parameters of the model jointly keeping the mask fixed, similar to [4], this avoids drift.

The overall optimization is outlined in Fig. 2. In this example, tokens [v1], [v2], and [v3] are assigned to the two subjects and a background of the second image respectively. With a good initialization of the token embeddings, we obtain the initial masks of the three concepts by averaging the attention maps over certain timesteps. Following this, we apply \mathcal{L}_{Mask} and \mathcal{L}_{attn} to update the tokens constrained by the given masks. With the newly updated tokens, we update the model weights to get an updated, better-quality mask. We repeat this process over a fixed number of steps (usually 400). At each iteration, we sample the timesteps to use for the update, similar to [4].

In this way, our approach can disentangle and learn concepts from a single image with masks generated during optimization. As illustrated in Fig. 3, the IoU of our optimized masks with respect to the ground-truth masks consistently increases for different concepts compared to the masks obtained from baseline (without optimization). Our approach thus provides flexibility to extract complex concepts without the requirement of a user-defined ground-truth mask.



Fig. 4: Qualitative results for concept-driven image generation. Here, we show a comparison between our results with mask optimization, baseline method without mask optimization, and ground truth approach.

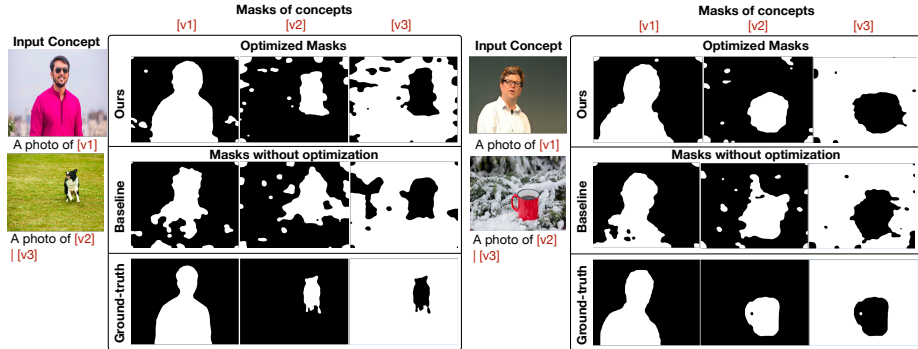


Fig. 5: Comparison of generated masks. Here we show user-defined masks, masks generated by the baseline method, and those produced by our approach. Note the significant improvement of the mask as a result of joint optimization (first row).

4 Experimental Results

In this section, we will show the experimental results through both quantitative measurements and qualitative assessments. Additionally, we conduct comparisons with baselines for a comprehensive evaluation.

Baseline Methods. We consider two baselines for comparing our proposed subject-driven image generation method, both of which are subsets of the Break-A-Scene [4]. These subsets involve: (1) utilizing user-defined masks (*i.e. ground truth masks*) and (2) operating without user-defined masks, which is a weakly supervised baseline (*baseline method*) to compare with our method. In this specific baseline approach, we create initial masks by aggregating attention maps derived from a pre-trained stable diffusion [46] model using 50 timesteps, rather than relying on ground truth masks. However, there is no optimization of these initial masks in the baseline method. We note that (1), which uses human-annotated perfect masks to delineate concepts, is a natural upper bound for our method. That said, it is possible in certain cases for us to outperform it as full-mask may not be optimal for learning the concept in question; the learned (latent) mask allows added flexibility in this respect. **Quantitative Comparison.** We con-

Table 1: Quantitative evaluation in terms of image similarity and diversity on COCO dataset.

Method	Cosine similarity(↑)	Clip similarity(↑)	LPIPS diversity (↑)
Baseline	0.8245	0.8987	0.3972
Ours (w/ aug)	0.81245	0.8960	0.4134
Ours (w/o aug)	0.8342	0.9062	0.40

Table 2: Quantitative evaluation based on user study.

Data	Baseline	Neutral	Ours
Random	10.92%	17.29%	71.80%
COCO	21.87%	18.69%	59.44%

sider three evaluation metrics to evaluate the faithfulness of the concept-driven generated images approach to the input concepts, considering two measurement criteria as follows:

- Similarity of the generated images: We use CLIP [42] and Cosine Similarity [32] scores to evaluate the resemblance of the generated images to the target images in terms of semantic similarity. Given a generated image, we use a pre-trained object detector (*e.g. YOLOv8* [24]) to detect the object of interest (corresponding to the input concept) in the generated image and compare their similarity to the target object from MSCOCO images. Table 1 displays the results for the baseline method and our method using CLIP and cosine similarity.
- Diversity between the generated images: We also consider how diverse the generated images for visual concept-driven generation are for a given prompt by comparing them using LPIPS [58] across different samples in the Table 1.

In Table 1, we present results on the COCO dataset [34]. We randomly selected 120 concepts from 11 COCO object classes, and generated them in various settings using 20 prompts each, creating 8 images for each prompt. We consider our approach with and without data augmentation. Data augmentation makes the generated images more diverse, but it can lead to lower similarity scores when compared to the target images. To account for this, similar to the baseline, we also evaluate our method without data augmentation and calculate semantic similarity using CLIP and cosine similarity scores. Our method without augmentation still performs better in diversity, due to EM-like optimization, allowing it to generate a wider variety of images compared to the baseline. This shows the importance of mask optimization in the process of generating masks.

Moreover, we also found human evaluation to be the best possible way to validate the approach. We randomly select 10 prompts and generate 6 images for each of them. We carried out a forced-choice experiment involving 11 participants to compare the generated images between our method and the baseline approach. These images were assessed for faithfulness to the target instance and the prompt



Fig. 6: Qualitative results demonstrating the interaction between different concepts. Here we present the interaction between newly learned concepts and the pre-existing concepts already familiar to the stable diffusion model.

condition (representing instances, contexts, and interactions) used to generate the images. As shown in Table 2, our method was preferred 71.8% of the time and was considered on par 17.29%. In addition, we conducted another, much larger scale one, using COCO in the same setting as in Tab. 1. In a user study with 17 participants, our approach was chosen 59.44% of the time, compared to

the baseline. This clearly illustrates the preference for results obtained using the joint token-mask optimization we propose.



Fig. 7: Diverse images for the same prompt. Given input concepts, our method demonstrates the ability to generate a variety of diverse outputs for a single prompt.

Qualitative Comparisons. Figure 4 shows the results of concept-driven image generation using our method, ground-truth (GT) [4], and the baseline method. The bottom rows exhibit the ground-truth masks, the respective learned concepts from two different use cases, and the images generated for interactions with multiple concepts. The middle rows and the top rows showcase the weakly supervised generated masks using the baseline and our method, respectively. In comparison to the baseline, our approach yields images that faithfully represent each concept in multi-concept image generation.

Figure 5 shows qualitative comparisons between the user-defined ground truth masks and the masks generated by both the baseline method and our approach. We can see that our optimized masks outperform the baseline masks without any optimization.

Additional Results. In Figure 6, we present the comparative results to show the interaction between newly introduced concepts and the pre-existing ones within the stable diffusion model. Our proposed method is not only able to interact between multiple concepts but also shows its capability to produce diverse outputs for a single prompt, as illustrated in Figure 7.

Furthermore, we demonstrate (in Figure 8) that our approach can interact within a cartoon world context as well. In this scenario, the pre-existing characters (*e.g.* Obama and Trump) are also depicted in a cartoon-like appearance.

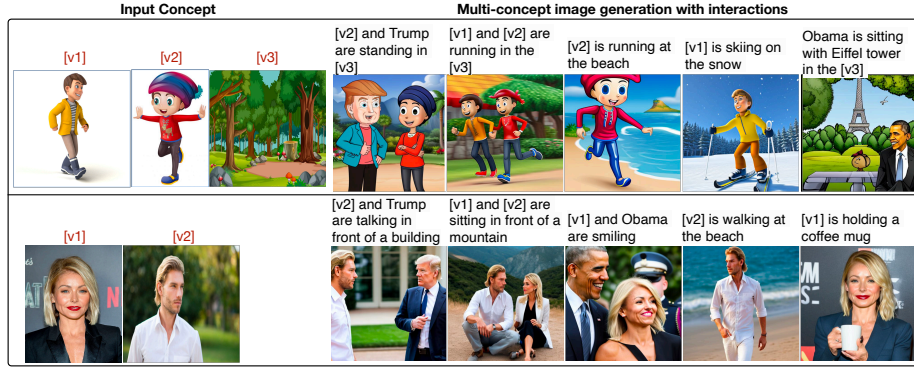


Fig. 8: Interaction between cartoon or real concepts ((including background)). Here, our method is not only able to interact with newly learned concepts but also engage with pre-existing concepts (such as Obama and Trump) in a cartoon-like appearance.

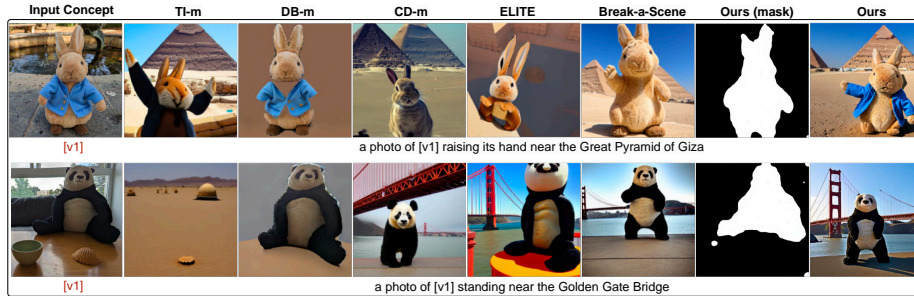


Fig. 9: Comparison of our method with standard baselines. Here we consider TI-m [13], DB-m [47], CD-m [31], ELITE [53], Break-a-scene [4] as standard baseline methods and all images are taken directly from [4].

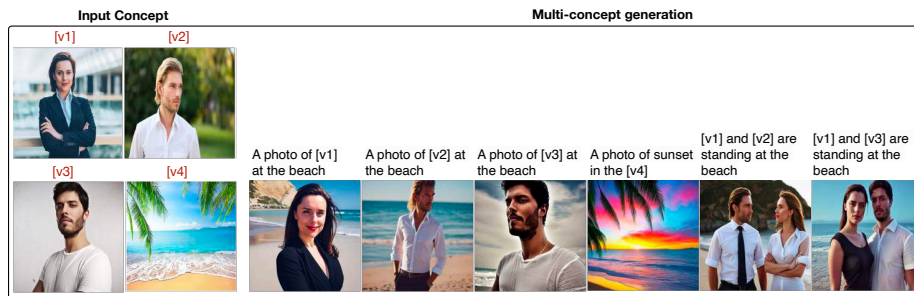


Fig. 10: Qualitative results show that our model can handle four concepts simultaneously.

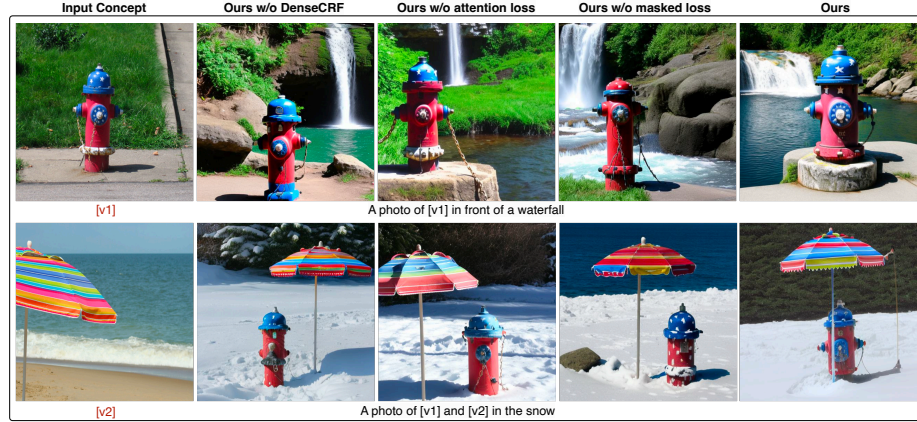


Fig. 11: Qualitative ablation by removing different components.

Besides, apart from lexical and cartoon concepts, we conduct experiments utilizing real-world concepts and show that our approach can generate multi-concept interactions between pre-existing and new concepts. We compare the qualitative results of our method in Figure 9. The comparative images are taken directly from Break-a-Scene [4]. We can see that our method can generate a better-optimized mask without any spatial supervision. Additionally, the generated images are more aligned with specific subjects and adhere more closely to the provided text prompts.

As an additional experiment, we conduct experiments to see if our model can learn more than three concepts (*e.g.*, four concepts), and the qualitative results are shown in Figure 10. We can see that our method excels in learning individual concepts but encounters challenges in effectively capturing interactions between these concepts. A possible extension of our proposed approach could address this limitation, and improve the approach to capture interactions between different concepts. Additional results are provided in the Supplemental.

Ablation Studies. To assess the contribution of each component, we conduct qualitative ablation by removing DenseCRF refinement, cross-attention loss, and masked diffusion loss in Figure 11. We can see that when we remove one of the components, the model tends to entangle concepts. Similar behavior has been observed in [4] for masked diffusion and cross-attention loss. Moreover, adding DenseCRF refinement improves the generated masks by 5.9% in terms of IOU.

5 Conclusion

We present an approach for generating multiple subjects with interconnections to facilitate personalized generation, even incorporating entities beyond out-of-distribution. Our method involves an alternating optimization method aimed at separating different concepts within a single image by producing masks tailored to distinct target concepts. We anticipate its role as a foundational element in the evolution of generative AI, further expanding the horizons of creative expression.

References

1. Abdal, R., Qin, Y., Wonka, P.: Image2stylegan: How to embed images into the stylegan latent space? In: ICCV (2019) [4](#), [5](#)
2. Abdal, R., Qin, Y., Wonka, P.: Image2stylegan++: How to edit the embedded images? In: CVPR (2020) [4](#)
3. Abdal, R., Zhu, P., Femiani, J., Mitra, N., Wonka, P.: Clip2stylegan: Unsupervised extraction of stylegan edit directions. In: SIGGRAPH (2022) [4](#)
4. Avrahami, O., Aberman, K., Fried, O., Cohen-Or, D., Lischinski, D.: Break-a-scene: Extracting multiple concepts from a single image. arXiv preprint arXiv:2305.16311 (2023) [2](#), [3](#), [7](#), [8](#), [10](#), [12](#), [13](#), [14](#)
5. Brock, A., Donahue, J., Simonyan, K.: Large scale gan training for high fidelity natural image synthesis. arXiv preprint arXiv:1809.11096 (2018) [4](#)
6. Chefer, H., Alaluf, Y., Vinker, Y., Wolf, L., Cohen-Or, D.: Attend-and-excite: Attention-based semantic guidance for text-to-image diffusion models. ACM Transactions on Graphics (TOG) **42**(4) (2023) [4](#)
7. Chen, H., Zhang, Y., Wang, X., Duan, X., Zhou, Y., Zhu, W.: Disenbooth: Identity-preserving disentangled tuning for subject-driven text-to-image generation. arXiv preprint arXiv:2305.03374 (2023) [4](#)
8. Chen, M., Radford, A., Child, R., Wu, J., Jun, H., Luan, D., Sutskever, I.: Generative pretraining from pixels. In: ICML (2020) [4](#)
9. Cohen, N., Gal, R., Meirom, E.A., Chechik, G., Atzmon, Y.: “this is my unicorn, fluffy”: Personalizing frozen vision-language representations. In: ECCV (2022) [4](#)
10. Dhariwal, P., Nichol, A.: Diffusion models beat gans on image synthesis. NeurIPS (2021) [4](#)
11. Esser, P., Rombach, R., Ommer, B.: Taming transformers for high-resolution image synthesis. In: CVPR (2021) [4](#)
12. Fei, Z., Fan, M., Huang, J.: Gradient-free textual inversion. arXiv preprint arXiv:2304.05818 (2023) [4](#)
13. Gal, R., Alaluf, Y., Atzmon, Y., Patashnik, O., Bermano, A.H., Chechik, G., Cohen-Or, D.: An image is worth one word: Personalizing text-to-image generation using textual inversion. arXiv preprint arXiv:2208.01618 (2022) [2](#), [4](#), [13](#)
14. Goodfellow, I., Pouget-Abadie, J., Mirza, M., Xu, B., Warde-Farley, D., Ozair, S., Courville, A., Bengio, Y.: Generative adversarial nets. NIPS (2014) [4](#)
15. Gu, J., Shen, Y., Zhou, B.: Image processing using multi-code gan prior. In: CVPR (2020) [5](#)
16. Gu, S., Chen, D., Bao, J., Wen, F., Zhang, B., Chen, D., Yuan, L., Guo, B.: Vector quantized diffusion model for text-to-image synthesis. In: CVPR (2022) [4](#)
17. Gu, Y., Wang, X., Wu, J.Z., Shi, Y., Chen, Y., Fan, Z., Xiao, W., Zhao, R., Chang, S., Wu, W., et al.: Mix-of-show: Decentralized low-rank adaptation for multi-concept customization of diffusion models. arXiv preprint arXiv:2305.18292 (2023) [5](#)
18. Han, I., Yang, S., Kwon, T., Ye, J.C.: Highly personalized text embedding for image manipulation by stable diffusion. arXiv preprint arXiv:2303.08767 (2023) [2](#), [4](#)
19. Han, L., Li, Y., Zhang, H., Milanfar, P., Metaxas, D., Yang, F.: Svdiff: Compact parameter space for diffusion fine-tuning. arXiv preprint arXiv:2303.11305 (2023) [4](#)
20. He, X., Cao, Z., Kolkin, N., Yu, L., Rhodin, H., Kalarot, R.: A data perspective on enhanced identity preservation for diffusion personalization. arXiv preprint arXiv:2311.04315 (2023) [4](#)

21. Ho, J., Jain, A., Abbeel, P.: Denoising diffusion probabilistic models. NeurIPS (2020) **4**
22. Ho, J., Saharia, C., Chan, W., Fleet, D.J., Norouzi, M., Salimans, T.: Cascaded diffusion models for high fidelity image generation. JMLR **23**(1), 2249–2281 (2022) **4**
23. Hu, E.J., Shen, Y., Wallis, P., Allen-Zhu, Z., Li, Y., Wang, S., Wang, L., Chen, W.: Lora: Low-rank adaptation of large language models. arXiv preprint arXiv:2106.09685 (2021) **4**
24. Inui, A., Mifune, Y., Nishimoto, H., Mukohara, S., Fukuda, S., Kato, T., Furukawa, T., Tanaka, S., Kusunose, M., Takigami, S., et al.: Detection of elbow ocd in the ultrasound image by artificial intelligence using yolov8. Applied Sciences (2023) **10**
25. Karras, T., Laine, S., Aila, T.: A style-based generator architecture for generative adversarial networks. In: CVPR (2019) **4**
26. Karras, T., Laine, S., Aittala, M., Hellsten, J., Lehtinen, J., Aila, T.: Analyzing and improving the image quality of stylegan. In: CVPR (2020) **4**
27. Kim, G., Kwon, T., Ye, J.C.: Diffusionclip: Text-guided diffusion models for robust image manipulation. In: CVPR (2022) **4**
28. Kim, G., Ye, J.C.: Diffusionclip: Text-guided image manipulation using diffusion models (2021) **4**
29. Kingma, D.P., Welling, M., et al.: An introduction to variational autoencoders. Foundations and Trends® in Machine Learning **12**(4), 307–392 (2019) **4**
30. Krähenbühl, P., Koltun, V.: Efficient inference in fully connected crfs with gaussian edge potentials. In: NIPS (2011) **7**
31. Kumari, N., Zhang, B., Zhang, R., Shechtman, E., Zhu, J.Y.: Multi-concept customization of text-to-image diffusion. In: CVPR (2023) **4, 13**
32. Lahitani, A.R., Permanasari, A.E., Setiawan, N.A.: Cosine similarity to determine similarity measure: Study case in online essay assessment. In: 2016 4th International Conference on Cyber and IT Service Management. IEEE (2016) **10**
33. Li, B., Qi, X., Lukasiewicz, T., Torr, P.: Controllable text-to-image generation. NIPS (2019) **4**
34. Lin, T.Y., Maire, M., Belongie, S., Hays, J., Perona, P., Ramanan, D., Dollár, P., Zitnick, C.L.: Microsoft coco: Common objects in context. In: ECCV. Springer (2014) **11**
35. Liu, Z., Feng, R., Zhu, K., Zhang, Y., Zheng, K., Liu, Y., Zhao, D., Zhou, J., Cao, Y.: Cones: Concept neurons in diffusion models for customized generation. arXiv preprint arXiv:2303.05125 (2023) **5**
36. Ma, J., Liang, J., Chen, C., Lu, H.: Subject-diffusion: Open domain personalized text-to-image generation without test-time fine-tuning. arXiv preprint arXiv:2307.11410 (2023) **4**
37. Nichol, A., Dhariwal, P., Ramesh, A., Shyam, P., Mishkin, P., McGrew, B., Sutskever, I., Chen, M.: Glide: Towards photorealistic image generation and editing with text-guided diffusion models. arXiv preprint arXiv:2112.10741 (2021) **4**
38. Nichol, A.Q., Dhariwal, P.: Improved denoising diffusion probabilistic models. In: ICML. PMLR (2021) **4**
39. Nitzan, Y., Aberman, K., He, Q., Liba, O., Yarom, M., Gandelsman, Y., Mosseli, I., Pritch, Y., Cohen-Or, D.: Mystyle: A personalized generative prior. ACM Transactions on Graphics (TOG) **41**(6) (2022) **4**
40. Van den Oord, A., Kalchbrenner, N., Espeholt, L., Vinyals, O., Graves, A., et al.: Conditional image generation with pixelcnn decoders. NeurIPS (2016) **4**
41. Parmar, N., Vaswani, A., Uszkoreit, J., Kaiser, L., Shazeer, N., Ku, A., Tran, D.: Image transformer. In: ICML (2018) **4**

42. Radford, A., Kim, J.W., Hallacy, C., Ramesh, A., Goh, G., Agarwal, S., Sastry, G., Askell, A., Mishkin, P., Clark, J., et al.: Learning transferable visual models from natural language supervision. In: ICML (2021) **4, 10**
43. Ramesh, A., Dhariwal, P., Nichol, A., Chu, C., Chen, M.: Hierarchical text-conditional image generation with clip latents. arXiv preprint arXiv:2204.06125 **1(2)** (2022) **4**
44. Ramesh, A., Pavlov, M., Goh, G., Gray, S., Voss, C., Radford, A., Chen, M., Sutskever, I.: Zero-shot text-to-image generation. In: ICML. PMLR (2021) **4**
45. Richardson, E., Alaluf, Y., Patashnik, O., Nitzan, Y., Azar, Y., Shapiro, S., Cohen-Or, D.: Encoding in style: a stylegan encoder for image-to-image translation. In: CVPR (2021) **5**
46. Rombach, R., Blattmann, A., Lorenz, D., Esser, P., Ommer, B.: High-resolution image synthesis with latent diffusion models. In: CVPR (2022) **1, 3, 4, 5, 10**
47. Ruiz, N., Li, Y., Jampani, V., Pritch, Y., Rubinstein, M., Aberman, K.: Dreambooth: Fine tuning text-to-image diffusion models for subject-driven generation. In: CVPR (2023) **2, 4, 13**
48. Saharia, C., Chan, W., Chang, H., Lee, C., Ho, J., Salimans, T., Fleet, D., Norouzi, M.: Palette: Image-to-image diffusion models. In: SIGGRAPH (2022) **4**
49. Tov, O., Alaluf, Y., Nitzan, Y., Patashnik, O., Cohen-Or, D.: Designing an encoder for stylegan image manipulation. ACM Transactions on Graphics (TOG) **40**(4) (2021) **5**
50. Vahdat, A., Kautz, J.: Nvae: A deep hierarchical variational autoencoder. NeurIPS (2020) **4**
51. Vaswani, A., Shazeer, N., Parmar, N., Uszkoreit, J., Jones, L., Gomez, A.N., Kaiser, Ł., Polosukhin, I.: Attention is all you need. NeurIPS **30** (2017) **4**
52. Wang, X., Girdhar, R., Yu, S.X., Misra, I.: Cut and learn for unsupervised object detection and instance segmentation. In: CVPR. pp. 3124–3134 (2023) **7**
53. Wei, Y., Zhang, Y., Ji, Z., Bai, J., Zhang, L., Zuo, W.: Elite: Encoding visual concepts into textual embeddings for customized text-to-image generation. arXiv preprint arXiv:2302.13848 (2023) **13**
54. Wu, W., Zhao, Y., Shou, M.Z., Zhou, H., Shen, C.: Diffumask: Synthesizing images with pixel-level annotations for semantic segmentation using diffusion models. arXiv preprint arXiv:2303.11681 (2023) **3, 6**
55. Xia, W., Zhang, Y., Yang, Y., Xue, J.H., Zhou, B., Yang, M.H.: Gan inversion: A survey. TPAMI **45**(3) (2022) **5**
56. Xie, J., Li, Y., Huang, Y., Liu, H., Zhang, W., Zheng, Y., Shou, M.Z.: Boxdiff: Text-to-image synthesis with training-free box-constrained diffusion. In: ICCV (2023) **4**
57. Yang, J., Wang, H., Xiao, R., Wu, S., Chen, G., Zhao, J.: Controllable textual inversion for personalized text-to-image generation. arXiv preprint arXiv:2304.05265 (2023) **2, 4**
58. Zhang, R., Isola, P., Efros, A.A., Shechtman, E., Wang, O.: The unreasonable effectiveness of deep features as a perceptual metric. In: CVPR (2018) **10**
59. Zhou, Y., Zhang, R., Chen, C., Li, C., Tensmeyer, C., Yu, T., Gu, J., Xu, J., Sun, T.: Lafite: Towards language-free training for text-to-image generation. arxiv 2021. arXiv preprint arXiv:2111.13792 **4**
60. Zhu, J., Shen, Y., Zhao, D., Zhou, B.: In-domain gan inversion for real image editing. In: ECCV. Springer (2020) **5**
61. Zhu, J.Y., Krähenbühl, P., Shechtman, E., Efros, A.A.: Generative visual manipulation on the natural image manifold. In: ECCV (2016) **5**

62. Zhu, P., Abdal, R., Qin, Y., Femiani, J., Wonka, P.: Improved stylegan embedding:
Where are the good latents? arXiv preprint arXiv:2012.09036 (2020) 5